

NUMERICAL STUDY OF THE SUPERSONIC FLOW AROUND WINGS

G. P. Voskresensky

Institute of Applied Mathematics
of the USSR Academy of Sciences, Moscow

Abstract

This paper deals with some computation results of the supersonic flow around flat wings and wings with airfoil. The wings have delta and other planforms and sharp and blunt leading edges. The flow fields around the wings were computed with the help of numerical algorithms. These algorithms of the second-order of accuracy were based on the finite-difference method of the solution of the problems for non-linear gasdynamic equations. The algorithms are suitable for the flow fields with detached and attached shock wave to the leading edge. The given examples consider the flow around the wings similar in planform but different in airfoils or in the position of the bow shock. The flow field on the upper surface of the flat delta wings and delta wings with airfoil are also considered. The lift coefficient for delta wings calculated according to the linear theory are estimated. The flow field around the wing of elliptical planform with detached shock wave and subsonic domain is represented.

Introduction

The aerodynamic design process of the wings of supersonic vehicles is becoming more complicated from year to year. A thorough study of the flow field around the wing for the given supersonic range is necessary. Besides some compromise must be found with subsonic and landing speeds of the vehicles. Now the wind tunnel experiments cannot satisfy scientists and engineers. It takes a long time to build mo-

del and the cost of the experiment is high, besides, even at moderate supersonic speeds such experiments don't furnish complete information. Some phenomena of the flow field around vehicles cannot be investigated in wind tunnels at all. All this stimulated the development of different numerical methods of the supersonic flow simulation. With the increase of the computer speed such methods are becoming an effective instrument for the computation of the flow and heat fields around vehicles. The more so, that the physical pattern of the flow field and its adequate mathematical description are authentic. Models of inviscid flow boundary layer which are used here are valid. Flow fields, shock waves, lift coefficients, pressure drag are determined within the framework of inviscid flow; heat fields and friction drag are determined within the framework of boundary layer.

A number of results obtained by the author at different times shows the efficiency of numerical methods in the detailed study of the supersonic flow field around wings. The examples refer to the inviscid flow and were computed with numerical algorithms. These algorithms are based on the implicit finite-difference schemes of the solution of continual differential equations with the second-order accuracy. The shape of wing surface may be constructively arbitrary. The shock wave is attached to the sharp leading edge or is detached from the blunt one. Much information about three-dimensional flow fields can be obtained with the help of

these algorithms but the descriptive and compact representation of this information presents great difficulties. That is why only typical information is given in the examples.

I

In the upper drawing of Figure I to the right of axis X , the upper side of the delta wing with the angle of sweep $\chi = 45^\circ$ and with the parabolic airfoil is shown. The relative thickness of the airfoil in its upper half is $\bar{c}_u = 0.05$. To the left of axis X , the upper side of the flat delta wing with the same planform is shown. The epures of the pressure on the surface of the wing with $M_\infty = 3.0$ and incidence $\alpha = 5^\circ$ are represented in four cross-sections of the wing with airfoil. The same epure for the flat delta wing is shown on the left hand side. (All epures in the cross-section of the flat delta wing are similar because the flow is automodelling). It can be seen that there is a considerable difference between the epures on the wing with airfoil and those on the flat wing. (1,2)

In the lower drawing of this Figure I the lower, windward side of this wing is shown. It also has a parabolical airfoil but with the relative thickness $\bar{c}_l = 0.04$. To the right of axis X on the lower side of this wing the epures of the pressure are represented. To the left of axis X the epure on the lower side of the flat wing is shown. A great difference in pressure distribution between the flat wing and the wing with airfoil can be seen. From here follows that in computing the aerodynamical loading on the delta wing it is necessary to take into consideration its airfoil. But the lift coefficients for the flat delta wing and for the wing with airfoil seem to be rather similar. For example the lift coefficients C_y for the delta wing with airfoil and for

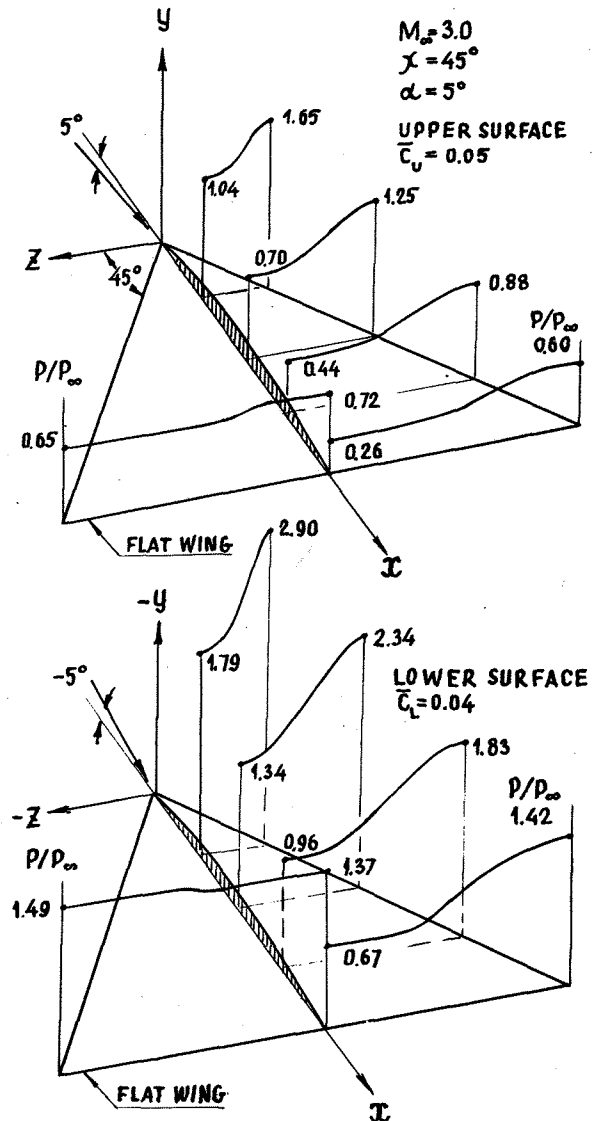


Figure I. The pressure distribution on the upper and lower sides of the delta wings.

flat delta wing at $\chi = 60^\circ$; $M_\infty = 4.0$ and $\alpha = 5^\circ$ are shown in the table.

	wing	flat wing	flat wing (lin.theor.)
C_y	0.086	0.091	0.090

The delta wing has a parabolical biconvex airfoil with the relative thickness of the upper part $\bar{c}_u = 0.05$ and of the lower part $\bar{c}_l = 0.02$. It can be seen that C_y

of the wing and of the plate are similar. The lift coefficient C_y for the flat delta wing computed by linear theory is also similar to them. Thus it is confirmed that the linear theory is suitable for approximate computation of C_y of the delta wing with airfoil with small angles of attack.

2

It is known, that the flow field on the leeward side of the flat delta wing is restricted not by the shock wave surface but by a conical characteristic surface because there is an expansion conical flow here. The numerical results show the flow streams from the right and left leading edges over flat wing meet and change the direction along the symmetry axis. This turn occurs in the conical embedded shock. The vortex of this conical shock surface coincides with the vortex of the flat delta wing. It is most intensive near the leeward side. Figure 2 shows the computed location of this embedded shock⁽³⁾ (circles) and the experimentally determined⁽⁴⁾ (lines) one.

There is no embedded shock if the upper side of the wing has the airfoil. It seems plausible that the turn of the stream to the symmetry axis is not so intensive as the one on the flat wing (in view of the complicated three-dimensional structure of the flow) and occurs without the formation of the internal shock.

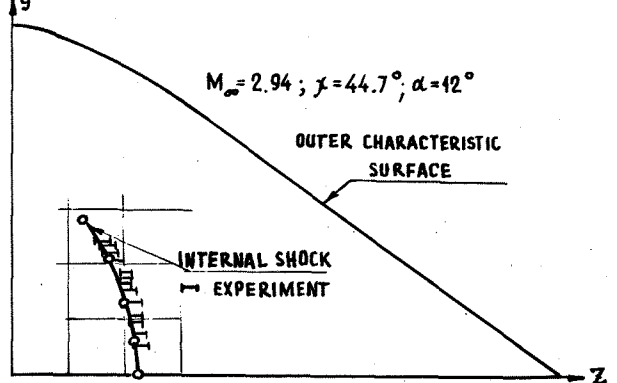


Figure 2. Location of the internal shock on the upper side of the flat delta wing.

In Figure 3 the loading distribution Δp computed⁽⁵⁾ for the delta wing with the sweep $\chi = 45^\circ$ and $M_\infty = 3.0$; $\alpha = 8^\circ$ is shown. The wing has the parabolic plane-convex airfoil with $\bar{c}_v = 0.05$. The location of the shock wave on the windward and leeward sides in four cross-sections is shown. On the leeward side near the tip of the wing the shock wave is transformed into an outer characteristic surface. This transition is shown with the crosses on the shock wave. The curve of the pressure behind the shock wave is shown in this Figure 3 by dash lines. It can be seen that the pressure near the tip of the wing is equal to one, i.e. to the pressure in free-stream. It is evi-

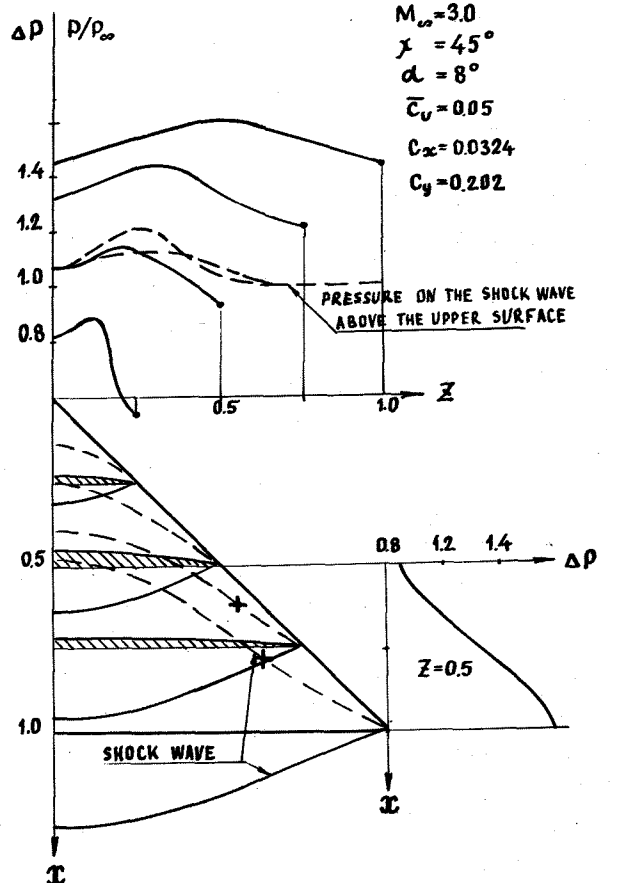


Figure 3. Loading distribution and the shock wave. The delta wing with plane-convex airfoil.

dence of the transition of the shock wave

into the outer characteristic surface.

The aerodynamical loading in longitudinal section of the wing with $Z = 0.5$ is represented separately. It increases towards the trailing edge of the wing.

The loading distribution for the delta wing with biconvex airfoil ($\bar{C}_y = 0.05$; $\bar{C}_L = 0.03$) and with the same parameters is computed. It is shown in Figure 4.

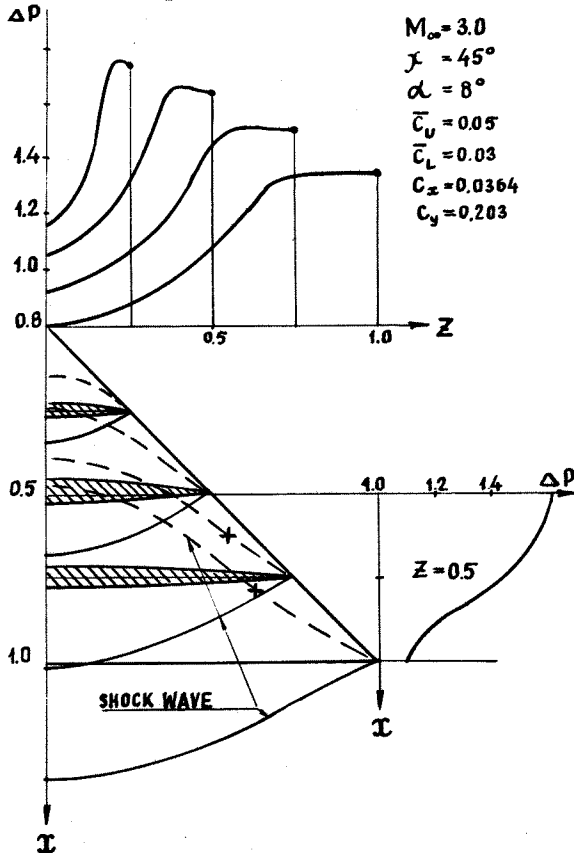


Figure 4. Loading distribution and the shock wave. The delta wing with biconvex airfoil.

The location of the shock wave in four cross-sections of the wing is also shown. The transition of the shock wave on the leeward side into outer characteristic surface also is shown with crosses on the shock wave. The aerodynamical loading in longitudinal section with $Z = 0.5$ is shown separately. It should be noted that the curve of the loading is quite different from the preceding wing. It decreases

towards the trailing edge of the wing. This different character of the aerodynamical loading of the delta wing with plane-convex airfoil and the one of the wing with biconvex airfoil indicates a great importance of the lower surface form of the wing at supersonic velocities. That is why the conclusions concerning the aerodynamical characteristics are made on the basis of the analysis of the flow field around the middle surface of the wing only may be groundless.

4

The shock wave is detached from the blunt leading edge of the wing with airfoil. An example of the flow field calculation around deltaplane⁽⁶⁾ with $M_\infty = 3.0$ and $\alpha = 5^\circ$ and with planform similar to the delta wing is shown in Figure 5.

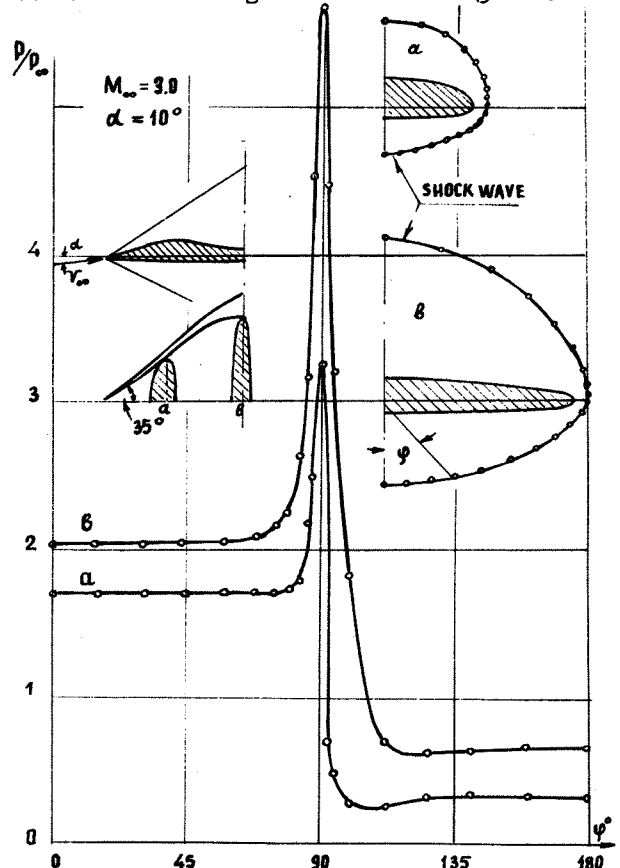


Figure 5. Pressure distribution on the deltaplane.

Also are shown its longitudinal section and planform. The pressure distribution on the surface and the form of the shock wave in two cross-sections are represented. The circles indicate the grid points. Attention should be paid to high gradient of pressure on the leading edge. In spite of the fact that the vehicle has great thickness, its lift coefficient C_y is rather similar to C_y of the flat delta wing with the same parameters of the free stream.

C_y of the deltaplane is 0.235 and C_y of the flat wing is 0.250. The divergence here is about 6%.

It should be noted that the lift coefficient C_y of a strongly flattened elliptical cone with the same vortex angle and the same free stream parameters is 17% higher than that of the flat wing. This takes place because the inclination of the lower surface of the elliptical cone is higher than the one at the deltaplane.

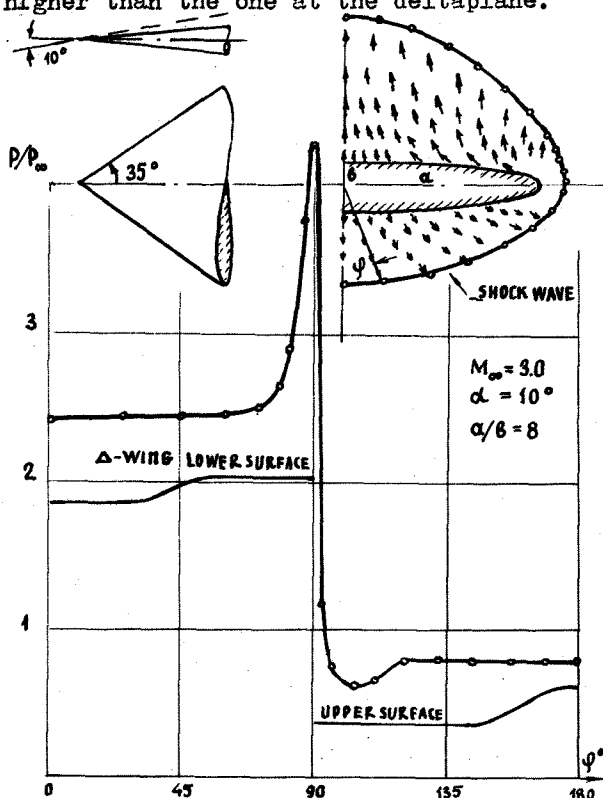


Figure 6. Pressure distribution on the elliptical cone and on flat wing.

Figure 6 shows the pressure distribution on the surface of this cone⁽⁶⁾. The shock wave and the value and position of the velocity vector in grid points of the flow field around this cone are shown in Figure 6 separately. The pressure on the lower and upper sides of the flat delta wing are represented for comparison.

5

The last example of the studies of the supersonic flow by the numerical methods refer to the flow on the front part of the wing with the detached shock wave. The flow fields with $M_\infty = 1.75$ and 1.5 around the front part of the wing with elliptical planform are considered here. The wing has small sweep angle and elliptical airfoil.

The difficulty of the numerical solution of this problem lies in the fact that there is a subsonic domain here with $M_\infty < 1$, and consequently the domain of the solution consists of subsonic and supersonic parts. (In all previous examples we dealt with supersonic domains only). In each of represented domains the flow field is described by its own kind of equations: by elliptical in the subsonic domain and by hyperbolic in the supersonic domain. For both parts the well-posed problems are different. A well-posed problem for the subsonic domain is the one with boundary conditions and for the supersonic domain it is the one with initial data. It is difficult to make a separate solution in both parts. That is why the problem is reduced to unsteady one that makes it possible to consider the problem from a single point of view.⁽⁷⁾ In this case the fourth additional coordinate of time is introduced and the equations are written in unsteady hyperbolic form. In this case the problem with the initial data is well-posed and the steady state is obtained as the asymptotic limit of an unsteady solution. The known time-dependent

stationing principle is used for this purpose. The introduction of an additional coordinate leads to a technological difficulty, but in principle, the problem becomes well defined and physically correct results may be expected from the solution.

Let us consider the computed flow without the details of the numerical solution. The flow field between the shock wave and the front part of the wing may be obtained. The positions of the detached shock wave and of the sonic surface are also determined. The sonic surface restricts the subsonic domain inside the flow field. The details of the flow field depend on the number of the grid points of the three-dimensional mesh. In the given example the number of the grid points was one thousand and one hundred. Figure 7 shows the general pattern of the flow field around the front part of an elliptical wing. The angle of attack of the wing is $\alpha = 5^\circ$.

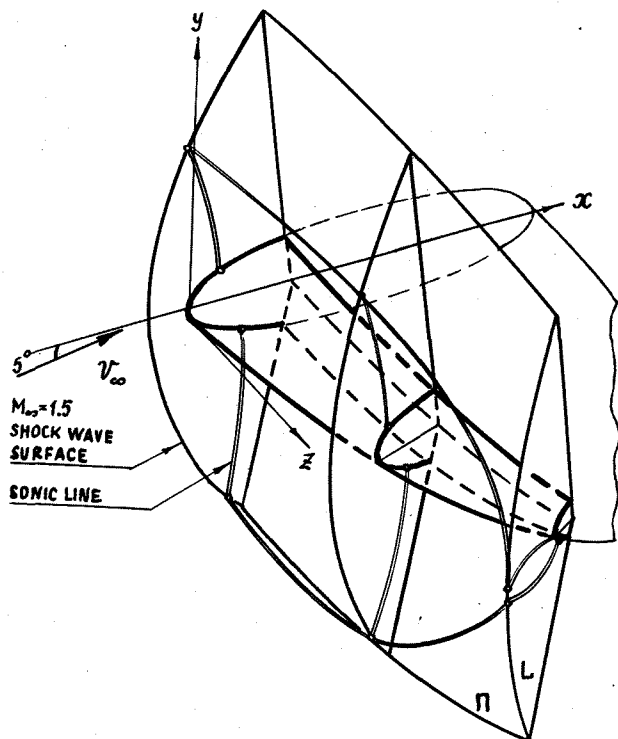


Figure 7. Pattern of the flow field around the front part of an elliptical wing.

The domain of the flow field is restricted by the surfaces of the wing and the shock wave (continuous lines). The subsonic domain is restricted by the sonic curves $M_w = 1$ (double lines). From behind and from side the computation domain is restricted by the planes Π and L . The flow field also is known on these planes.

The position and the value of the velocity vector in grid points between the wing surface and the shock wave in plane \mathcal{XOY} are shown in Figure 8. (An elliptical wing, $M_\infty = 1.75$; $\alpha = 5^\circ$).

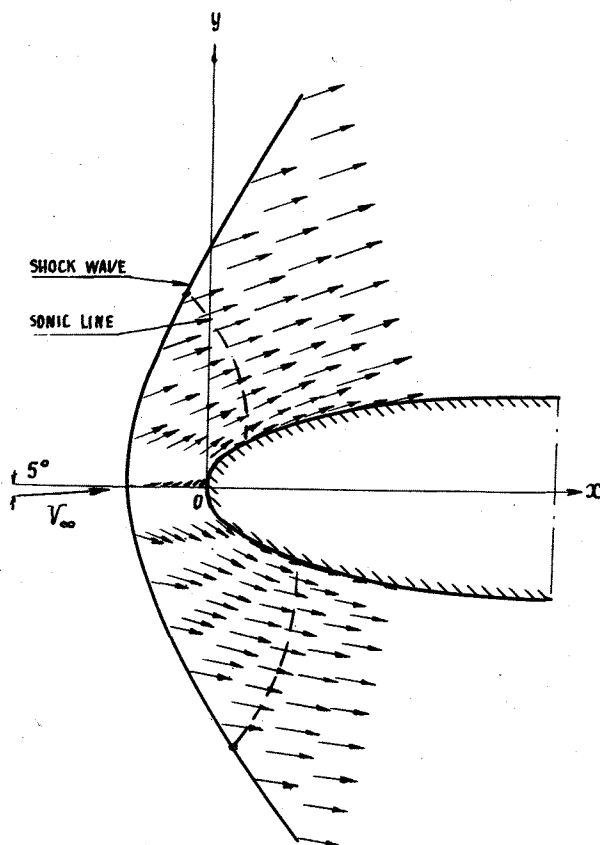


Figure 8. Flow field of the velocity vector. $M_\infty = 1.75$; $\alpha = 5^\circ$.

The sonic line restricts the subsonic domain. The flows above and below the wing influence each other through this subsonic domain. The flow directed from the lower to the upper side of the wing can be seen on axis \mathcal{X} .

References

1. Voskresensky G.P., Iljina A.S., Tatarenchik V.S. A supersonic flow around wings. Preprint. Inst. of Appl. Mathem. of the USSR Academy of Sciences, 1976, I04.
2. Voskresensky G.P., Iljina A.S., Tatarenchik V.S. A supersonic flow around wing with the attached shock wave. Trudi TSAGI, I590, 1974.
3. Voskresensky G.P. Numerical solution for the flow past upper surface of a delta wing in the expansion region. J. Prikladn. Mechan. i Techn. Phys. 6, 1973.
4. Bannink W.J., Nebbeling C. An experimental investigation of the expansion flow field over a delta wing at supersonic speed. Report VTH-I67, Delft University of Technology, Delft 1971.
5. Voskresensky G.P., Iljina A.S., Tatarenchik V.S. Supersonic flow around sharp tip wings. J. Prikladn. Mechan. i Techn. Phys. 6, 1977.
6. Voskresensky G.P., Tatarenchik V.S., Shepetievsky O.A. Supersonic flow around sharp and flattened bodies. Preprint. Inst. of Appl. Mathem. of the USSR Academy of Sciences, 1976, I6.
7. Voskresensky G.P., Ivanova V.N. Supersonic unsteady inviscid flow around front part of the wings with detached shock wave. Preprint. Inst. of Appl. Mathem. of the USSR Academy of Sciences 1977, I30.
8. Voskresensky G.P. Numerical solution for the flow past an arbitrary surface of a delta wing in the compression region. Izv. AN SSSR, Mechan. Zhidkosti i gaza, 4, 1968.